

CONF-8410142--24

Operations Division

CONF-8410142--26

DE85 002500

**LWR SURVEILLANCE DOSIMETRY IMPROVEMENT PROGRAM:
PSF METALLURGICAL BLIND TEST RESULTS***

F. B. K. Kam
R. E. Maerker
F. W. Stallmann

*Prepared for the
U.S. Nuclear Regulatory Commission
Office of Nuclear Regulatory Commission
Washington, D.C. 20555
under Interagency Agreements DOE 40-551-75 and 40-552-75

NRC FIN No. B0415

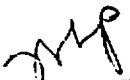
By acceptance of this article, the
publisher or recipient acknowledges
the U.S. Government's right to
retain a nonexclusive, royalty-free
license in and to any copyright
covering the article.

MASTER

Prepared by the
Oak Ridge National Laboratory
Oak Ridge, Tennessee 37830
operated by
MARTIN MARIETTA ENERGY SYSTEMS, INC.
for the
U.S. DEPARTMENT OF ENERGY
under Contract No. DE-AC05-84OR21400

**NOTICE
PORTIONS OF THIS REPORT ARE ILLEGIBLE**

as been reproduced from the best
able copy to permit the broadest
able availability.


DISTRIBUTION OF THIS DOCUMENT IS UNLIMITED

CONF-8410142

LWR SURVEILLANCE DOSIMETRY IMPROVEMENT PROGRAM:
PSF METALLURGICAL BLIND TEST RESULTS

F. B. K. Kam
R. E. Maerker
F. W. Stallmann

Oak Ridge National Laboratory
Oak Ridge, Tennessee 37831, U.S.A.

SUMMARY

The metallurgical irradiation experiment at the Oak Ridge Research Reactor Poolside Facility (ORR-PSF) was designed as a benchmark to test the accuracy of radiation embrittlement predictions in the pressure vessel wall of light water reactors on the basis of results from surveillance capsules. The ORR-PSF (Fig. 1) consists of the ORR reactor core and the ex-core components that are used to mock up pressure vessel surveillance configurations for light water reactors (LWRs). The ex-core components are the thermal shield (TS), the simulated surveillance capsule (SSC), the simulated pressure vessel capsule (SPVC), and the simulated reactor cavity [void box (V3)]. The aluminum window is part of the ORR pressure vessel which separates the core from the ex-core components. The PSF metallurgical Blind Test is concerned with the SSC and the SPVC. Five metallurgical specimen assemblies were prepared for the irradiation experiment. Each assembly contains the same mix of plate forging and weld material specimens. Dosimeters are distributed throughout each assembly to monitor the neutron exposure received by the specimens. Two capsules were fabricated for irradiation at the simulated surveillance location (SSC1 and SSC2) in sequence to fluences of 2×10^{19} and 4×10^{19} neutrons/cm², respectively. Each SSC contained one of the metallurgical specimen assemblies. The SPVC contained the other three assemblies which were positioned at locations corresponding to the inner surface (0-T), the quarter thickness (1/4 T), and the half thickness (1/2 T) of a pressure vessel. The fluences for SSC1 and SSC2 are approximately equal to the 1/4T and 0-T positions, respectively. The total irradiation times for SSC1 and SSC2 are approximately 46 days and 92 days while the irradiation time for the SPVC is approximately 600 days. The temperature of the specimens was tightly controlled to $288^\circ \pm 7^\circ\text{C}$ during the irradiation.

All capsules contained extensive dosimetry which was combined with neutron physics calculations in an adjustment procedure to determine a spatial map of damage parameter values at all metallurgical specimen locations including uncertainties. Computer fits to raw Charpy test data from the experiment were used to determine shifts of transition temperature (NDT) and upper shelf energy (USE) at the given fluences, again including uncertainties.

The data from the ORR-PSF benchmark experiment are the basis for comparison with the predictions made by participants of the metallurgical "Blind Test." The Blind Test required the participants to predict the embrittlement of the irradiated specimen based only on dosimetry and metallurgical data from the SSC1 capsule. This exercise included both the prediction of damage fluence and the prediction of embrittlement based on the predicted fluence. A variety of prediction methodologies was used by the participants. No glaring biases or other deficiencies were found, but neither were any of the methods clearly superior to the others.

Closer analysis shows a rather complex and poorly understood relation between fluence and material damage. Many prediction formulas can give an adequate approximation, but further improvement of the prediction methodology is unlikely at this time given the many unknown factors. Instead, attention should be focused on determining realistic uncertainties for the predicted material changes. The Blind Test comparisons provide some clues for the size of these uncertainties. In particular, higher uncertainties must be assigned to materials whose chemical composition lies outside the data set for which the prediction formula was obtained.

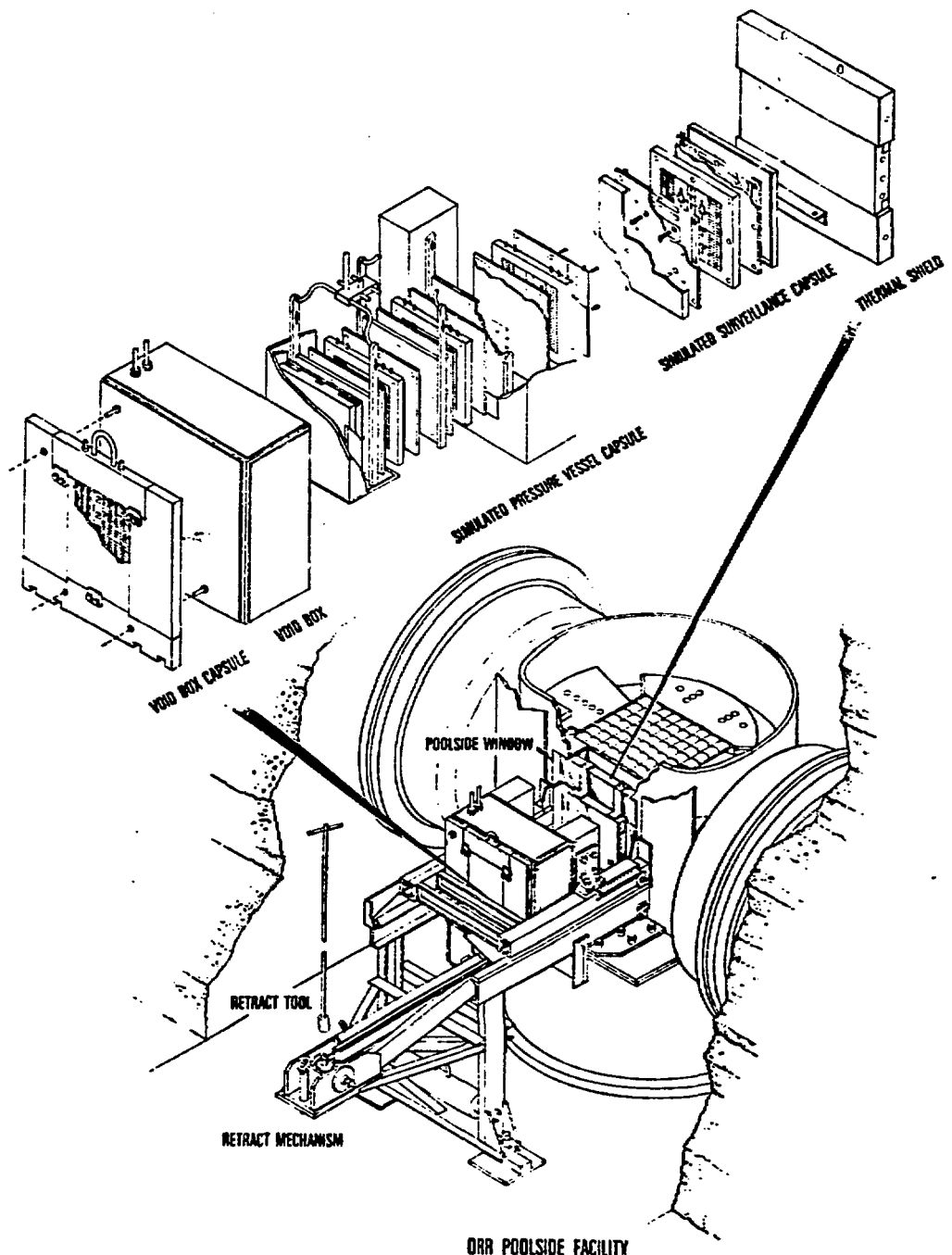


Fig. 1. ORR-PSF Irradiation Facility.

LWR SURVEILLANCE DOSIMETRY IMPROVEMENT PROGRAM:
PSF METALLURGICAL BLIND TEST RESULTS

F. B. K. Kam
R. E. Maerker
F. W. Stallmann

Oak Ridge National Laboratory
Oak Ridge, Tennessee 37831, U.S.A.

INTRODUCTION

The metallurgical irradiation experiment at the Oak Ridge Research Reactor Poolside Facility (ORR-PSF) is one of the series of benchmark experiments in the framework of the Light Water Reactor (LWR) Surveillance Dosimetry Improvement Program (Fig. 1). The goal of this program is to test, against well-established benchmarks, the methodology which is used to predict the irradiation embrittlement of pressure vessels in commercial power reactors at the end of their service life and to determine safe operating limits for these vessels. Knowledge of pressure vessel embrittlement is also essential to determine the resistance of the vessel under thermal shock conditions and to determine if and when annealing of the vessel is needed. The prediction methodology as practised in pressure vessel surveillance programs includes procedures for neutron physics calculations, dosimetry and spectrum adjustment methods, and metallurgical tests and damage correlation. The benchmark experiments in the framework of the Dosimetry Improvement Program serve to validate, improve, and standardize these procedures. The results of this program are implemented in a set of ASTM Standards (Fig. 2) on pressure vessel surveillance procedures, which are in various stages of completion.¹ These in turn may be used as guides for regulatory procedures of the Nuclear Regulatory Commission (NRC).

The ORR-PSF experiment was specifically designed to simulate the surveillance capsule-pressure vessel configuration in power reactors and to test the validity of procedures which determine the radiation damage in the vessel from test results of surveillance capsules. Emphasis was on radiation embrittlement of reactor vessel steels and damage correlation in order to test current embrittlement prediction methodologies. For this purpose, a PSF metallurgical Blind Test was initiated.² Experimental results were withheld from the participants; only the type of information which is normally contained in surveillance reports was given. The goal was to predict from this limited information the metallurgical test results in the pressure vessel wall capsule. Of particular interest was the question, what effects, if any, the differences in fluence rate and fluence spectrum in the surveillance capsule and in the pressure vessel wall may have on the embrittlement prediction.

DISCLAIMER

This report was prepared as an account of work sponsored by an agency of the United States Government. Neither the United States Government nor any agency thereof, nor any of their employees, makes any warranty, express or implied, or assumes any legal liability or responsibility for the accuracy, completeness, or usefulness of any information, apparatus, product, or process disclosed, or represents that its use would not infringe privately owned rights. Reference herein to any specific commercial product, process, or service by trade name, trademark, manufacturer, or otherwise does not necessarily constitute or imply its endorsement, recommendation, or favoring by the United States Government or any agency thereof. The views and opinions of authors expressed herein do not necessarily state or reflect those of the United States Government or any agency thereof.

To serve as a benchmark, a very careful characterization of the ORR-PSF experiment is necessary, both in terms of neutron fluence spectra and of metallurgical test results. Statistically determined uncertainties must be given in terms of variances and covariances to make the comparisons between predictions and experimental results meaningful. A description of the characterization program is given in the first part of this paper. The second part discusses the results of the Blind Test and its implications.

DESCRIPTION OF THE EXPERIMENT

The ORR-PSF (Fig. 3) consists of the ORR reactor core and the ex-core components that are used to mock up pressure vessel surveillance configurations for light water reactors (LWRs). The ex-core components are the thermal shield (TS), the simulated surveillance capsule (SSC), the simulated pressure vessel capsule (SPVC), and the simulated reactor cavity [void box (VB)]. The aluminum window is part of the ORR pressure vessel which separates the core from the ex-core components. The PSF metallurgical Blind Test is concerned with the SSC and the SPVC. Five metallurgical specimen assemblies were prepared for the irradiation experiment. Each assembly (Fig. 4) contains the same mix of plate forging and weld material specimens.^{3,4} Dosimeters are distributed throughout each assembly to monitor the neutron exposure received by the specimens. Two capsules were fabricated for irradiation in sequence at the simulated surveillance location (SSC1 and SSC2) to fluences of 2×10^{19} and 4×10^{19} neutrons/cm², respectively. Each SSC contained one of the metallurgical specimen assemblies. The SPVC contained the other three assemblies which were positioned at locations corresponding to the inner surface (0-T), the quarter thickness (1/4 T), and the half thickness (1/2 T) of a pressure vessel. The fluences for SSC1 and SSC2 are approximately equal to the 1/4T and 0-T positions, respectively. The total irradiation times for SSC1 and SSC2 are approximately 46 days and 92 days while the irradiation time for the SPVC is approximately 600 days. The temperature of the specimens was tightly controlled to $288^\circ \pm 7^\circ\text{C}$ during the irradiation (Ref. 5).

A "startup experiment" with dummy capsules containing only dosimeters was performed prior to the metallurgical experiment in order to determine accurately the irradiation times needed to reach the target fluences. This experiment was also used to test the accuracy of a preliminary neutron transport calculation. Comparison of dosimetry results between the startup and the two-year experiment showed significant differences, which were traced to differences in core loadings.^{6,7} A new set of transport calculations, described in the next section, was performed to account for 52 different core loadings.

NEUTRON TRANSPORT CALCULATION

Flux, fluence, and activity calculations were performed for each of the three exposures (two surveillance capsules and a pressure vessel capsule) performed during the two-year metallurgical Blind Test experiment at the ORR-PSF. Motivation for these calculations was prompted by differences of up to 25% between dosimetry measurements performed in the earlier startup scoping experiment and the two-year experiment.

Following the same simplified calculational methods used in a re-analysis of the startup experiment, fission source distributions were obtained from three-dimensional diffusion theory for most of the 52 cycles active during the course of the complete experiment, combined in small groups, and the resultant ex-core group fluxes calculated by two-dimensional discrete ordinate transport theory. More details can be found in Refs. 7 and 8.

Comparisons of the dosimeter end-of-irradiation activities with HEDL measurements indicate agreement generally within 15% for the first surveillance capsule, 5% for the second, and 10% for three locations in the pressure vessel capsule, which are as good as, if not somewhat better than, comparisons in the startup experiment. The calculations thus validate the trend of the measurements in both the startup and the two-year experiments and confirm the presence of a significant cycle-to-cycle variation in the core leakage. The tape containing the unadjusted spectral fluences for each of the three exposures that can be used in the metallurgical analysis is thus considered to be accurate to within about 10%.

DOSIMETRY AND ADJUSTMENT PROCEDURES

A 10% accuracy, as quoted in the preceding section, for the damage parameter values of the metallurgical specimen is quite sufficient for most metallurgical damage correlation studies. However, since the ORR-PSF experiment is intended as benchmark, higher accuracies and a more thorough study of the uncertainties is required. Thus, a comprehensive statistical analysis with the use of adjustment procedures was made resulting in a complete three-dimensional fluence map. This map includes not only the damage parameter values $\phi t > 1.0$ MeV, $\phi t > 0.1$ MeV (ϕt = fluence), and dpa, but values for all major threshold reactions. These were included to test dosimetry measurements from a variety of laboratories and some experimental dosimetry (e.g., damage monitors) which were not used in the adjustment procedure.

Details of the dosimetry in the ORR-PSF experiment are given in Ref. 9. The measurements, which are available to date, can be found in Refs. 7 and 10. Figure 5 gives an overview of the methodology used to obtain the three-dimensional fluence map.

The LSL-M2 adjustment procedure¹¹ was used for the evaluation. In it, data from the transport calculation were combined with the dosimetry from the gradient sets (GS), back bone sets (BB), and gradient strips along the Charpy specimens (see Fig. 4 and Ref. 9). Adjusted damage parameter values at capsule centers are listed in Table 1, together with uncertainties. Values at other positions of the capsules are determined through a cosine-exponential fit

$$P(X, Y, Z) = P_0 \cos B_X(X-X_0) \cos B_Z(Z-Z_0) e^{-\lambda(Y-Y_0)} \quad (1)$$

where $P(X, Y, Z)$ is the value of the damage parameter in question at (X, Y, Z) . (For the orientation of the coordinate system, see Fig. 6.) There is one set of fitting parameters for each capsule and each damage parameter. The values are listed in Table 2. This interpolation-extrapolation introduces additional uncertainties, which increase with increasing distance from the capsule centers, up to about 5%. More details can be found in Ref. 12.

STATISTICAL EVALUATION OF THE METALLURGICAL TESTS

The need for rigorous statistical evaluation of the experimental results is not restricted to dosimetry and neutron fluence determination. The high standard for accuracy and reliable determination of uncertainties apply also to the metallurgical test results. The primary source for the Blind Test comparisons are the results from the Charpy tests. The raw Charpy data⁴ are fitted to continuous curves, impact energy vs. test temperature, in order to determine the shift of nil-ductility temperature (Δ NDT) and upper shelf energy (Δ USE) with increasing damage fluence. Eyeball fits as used in Refs. 3 and 4 leave too much room for individual judgment and biases and cannot assign uncertainties to the resulting shifts. In the ORNL evaluation,¹³ a computer fit CV81* was used. This fitting procedure uses separate curves for NDT and USE and is, therefore, more flexible than hyperbolic tangent or error function approximations which are commonly used for computer fits. (These fits were used by some Blind Test participants.) There is no significant difference between the CV81 evaluations and the eyeball fits in Ref. 4, as can be seen in Table 5, but the statistical computer fit allows the calculation of uncertainties. Table 3 lists the different materials used in the metallurgical irradiation and their chemical composition. A summary of the CV81 results is given in Table 4. Details of the procedure are given in Ref. 13.

DISCUSSION OF THE BLIND TEST RESULTS

The participants of the Blind Test received the following information:

1. Calculated 102-group flux-spectrum, exposure rate parameters, and dosimeter reaction rates for the SSC1, SSC2, and SPVC 0-T PV surface, 1/4T wall, 1/2T wall, 3/4T wall, and SVBC positions. (This calculation is different from the one described in this paper, in that it was done for the "startup" experiment with somewhat different core configuration.)
2. The SSC1 measured in-situ dosimetry as-built information, exposure time history, and post-irradiation sensor results.
3. The SSC1, SSC2, and SPVC 0-T, 1/4T, and 1/2T measured in-situ Co-Al alloy bare and gadolinium-covered sensor results needed and used to determine two additional low-energy group flux-spectral values for the thermal and thermal to 9.8×10^{-2} MeV energy ranges.
4. The SSC1, SSC2, and SPVC measured metallurgical specimen exposure time histories.
5. The SSC1, SSC2, and SPVC measured metallurgical specimen temperature time histories.
6. The SSC1, SSC2, and SPVC as-built metallurgical specimen dimensional and placement information.
7. The SSC1 metallurgical specimen heat treatment, chemistry, and measured un-irradiated and irradiated properties for different steels.

*CV81 is a linear least squares procedure, although linear combinations of non-linear functions can be used.

Participants were asked to predict both the damage parameter values and the metallurgical test results in the SSC2 and SPVC capsules.

To determine damage parameter values, most participants used the calculated fluences normalized with measurements at the SSC1. Adjustment procedures and cosine-exponential fits were also used by some participants. Uncertainties were quoted by some participants which were all on the optimistic side. None of the quoted figures for damage parameter values differed by more than 30% in either direction from the ORNL evaluation, and 65% of the values were within $\pm 10\%$ of ORNL. Differences in the damage parameter determinations had very little impact on the determination of radiation damage. That is, some participants who predicted low damage parameter values quoted high embrittlement values and vice versa.

The prediction of materials property changes, primarily NDT and USE for Charpies vs. fluence, were all based on one of the two formulas

$$\Delta M = C (\phi t)^a \quad , \text{ or} \quad (2)$$

$$\Delta M = C (\phi t)^{(a-b \cdot \log(\phi t))} \quad (3)$$

with ΔM materials change and ϕt fluence > 1.0 MeV (or some other damage parameter such as dpa). C is a "chemistry factor" which is either determined explicitly from the chemical composition and a data base or used as a scale factor based on the SSC1 results. Formula (2) with $a = 0.5$ is used in NRC Reg. Guide 1.99.¹⁴ Other (usually smaller) values of a are used by some participants as obtained from their data bases. The "Guthrie formula" (3)¹⁵ replaces the straight line in a log-log plot by a parabola, taking into account that damage "saturates" faster than a single exponent would indicate. The parameters a and b were either the ones originally obtained by Guthrie or modifications obtained from their own data bases.

The 41J- RT_{NDT} results of the predictions are summarized in Table 5. Lowest and highest predictions are strikingly close to each other and mostly symmetrically distributed relative to the experimental values. The largest deviation, between measurements and prediction, is for the weld code (R) in the SPVC capsules. The high nickel content places this material outside the data bases from which the prediction formulas were obtained. Aside from this material, no consistent biases nor significant deviations between predictions and experimental values were found. Also, none of the prediction formulas were consistently superior.

The explanation for this outcome can be found in the graphs, Figs. 7-12, which plot the experimental shifts against the damage parameter dpa. The data points for each of these graphs can be fitted to a variety of straight lines (2) or slightly curved parabolas (3) within the indicated uncertainty bounds. Since the actual curves for different materials show quite different slopes and curvatures, no single formula will give a good fit for all of them. On the other hand, large uncertainties and variability within the material, due to such factors as heat treatment or position and direction of the specimen, make it unlikely that further improvement is possible beyond the simple approximations (2) and (3).

Since the prediction accuracy is not likely to improve, realistic uncertainty bounds need to be provided with the predictions so that proper safety margins can be established. Only a few Blind Test participants gave uncertainties with their predictions and most were on the low side when compared with experimental values. The Blind Test comparisons in Table 5 give already some indications for the actual prediction uncertainties. More studies and more detailed analyses of existing data bases are needed to determine safe, but not overly conservative uncertainty bounds.

It is informative to compare the metallurgical results from the ORR-PSF experiment with the predictions of the old Reg. Guide 1.99,¹⁴ which is based on formula (2) and the proposed revision¹⁶ which is based on the Guthrie formula (3).¹⁵ The chemistry factor in the old Guide is a linear combination of copper and phosphorus, whereas the new version has the chemistry factor in tabular form with copper and nickel as entries, separate for plate materials and welds. By dividing the Charpy shift by the chemistry factor, all materials can be compared on the same basis having only one upper bound curve for all materials in either Reg. Guide. As the graph in Fig. 13 shows, the old Reg. Guide is not a good representation of correlation between chemistry, fluence, and NDT shift, since the data points are widely scattered both above and below the boundary line. The revised Guide shows much less scatter and data points from the same material appear to follow the Guthrie curve much better than the square root line in Fig. 13. A safety margin which was suggested in (18) was subtracted from the data in Fig. 14 so that most points now lie safely below the boundary line. The two exceptions are the code (K) and (R) materials. Both have higher nickel content than any of the steels in the data base from which the chemistry table was generated.^{15,16} It follows that higher safety margins must be imposed on such materials. Or, alternatively, metallurgical irradiation experiments to several different fluences must be performed for such materials to determine the proper chemistry (normalization) factor.

CONCLUSIONS AND RECOMMENDATIONS

The PSF metallurgical Blind Test comparisons show that the various embrittlement prediction formulas are adequate as rough approximations, but that none captures the complex and not-well-understood correlation between radiation embrittlement and fluence, fluence rate, neutron spectrum, chemistry, heat treatment and, perhaps, other factors. None of the current prediction formulas appears clearly superior, but the Guthrie formula captures somewhat better the saturation effect at higher fluences, since the quadratic term adds more flexibility. Improvements are possible in the following areas:

1. Realistic uncertainties need to be established in conjunction with prediction formulas. The Blind Test comparison gives some clues for the size of uncertainties (Table 5). Larger data bases and statistical evaluations, which are more specifically directed towards uncertainties, are needed for more definite results.
2. Prediction formulas which were derived from a data base may not be valid for materials whose composition is outside the range of the data base. Substantially higher safety margins must be applied to such materials or test irradiations performed to establish trend curves for the particular material.

REFERENCES

1. ASTM Standard E706-81a, "Master Matrix for LWR Pressure Vessel Surveillance Standards," 1983 Annual Book of ASTM Standards, Vol. 12.2, American Society for Testing and Materials, Philadelphia, PA, 1983.
2. W. N. McElroy and F. B. K. Kam, eds., PSF Blind Test Instructions and Data Packages, distributed to Blind Test participants, March 22, 1983.
3. J. R. Hawthorne, B. H. Menke, and A. L. Hiser, Light Water Reactor Pressure Vessel Surveillance Dosimetry Improvement Program: Notch Ductility and Fracture Toughness Degradation of A 302-B and A 533-B Reference Plates from PSF Simulated Surveillance and Through-Wall Irradiation Capsules, NUREG/CR-3295, MEA-2017, Vol. 1, U.S. Nuclear Regulatory Commission, Washington, DC, 1983.
4. J. R. Hawthorne and B. H. Menke, Light Water Reactor Pressure Vessel Surveillance Dosimetry Improvement Program: Notch Ductility and Tensile Strength Determinations for PSF Simulated Surveillance and Through-Wall Irradiation Capsules, NUREG/CR-3295, MEA-2017, Vol. 2, U.S. Nuclear Regulatory Commission, Washington, DC, 1983.
5. L. F. Miller, Analysis of Temperature Data From the ORR-PSF Irradiation Experiment: Methodology and Computer Software, NUREG/CR-2273, ORNL/TM-7766, U.S. Nuclear Regulatory Commission, Washington, DC, 1981.
6. H. Tourwe, et al., "Interlaboratory Comparison of Fluence Neutron Dosimeters in the Frame of the PSF Start-Up Measurement Program, Proc. of the 4th ASTM-EURATOM Symposium on Reactor Dosimetry," Gaithersburg, MD, March 22-26, 1982, NUREG/CP-0029, Vol. 1, pp. 159-168, U.S. Nuclear Regulatory Commission, Washington, DC, 1982.
7. R. E. Maerker and B. A. Worley, Activity and Fluence Calculations for the Startup and Two-Year Irradiation Experiments Performed at the Poolside Facility, NUREG/CR-3886, ORNL/TM-9265, U.S. Nuclear Regulatory Commission, Washington, DC, 1984.
8. R. E. Maerker and B. A. Worley. "Calculated Spectral Fluences and Dosimeter Activities for the Metallurgical Blind Test Irradiations at the ORR-PSF," to be presented at the 5th ASTM-EURATOM Symposium on Reactor Dosimetry, Geesthacht, FRG, September 24-28, 1984.
9. E. P. Lippincott, et al., Fabrication Data Package for HEDL Dosimetry in the ORR Poolside Facility LWR Pressure Vessel Mock-Up Irradiation, HEDL-TC-2065, Hanford Engineering Development Laboratory, Richland, WA, 1981.
10. G. L. Guthrie, E. P. Lippincott, and E. D. McGarry, Light Water Reactor Pressure Vessel Surveillance Dosimetry Improvement Program: PSF Blind Test Workshop Minutes, Hanford Engineering Development Laboratory, Richland, WA, April 9-10, 1984.

11. F. W. Stallmann, "LSL-M1 and LSL-M2: Two Extensions of the LSL Adjustment Procedure for Including Multiple Spectrum Locations," to be presented at the 5th ASTM-EURATOM Symposium on Reactor Dosimetry, Geesthacht, FRG, September 24-28, 1984.
12. F. W. Stallmann, Determination of Damage Exposure Parameter Values in the PSF Metallurgical Irradiation Experiment, NUREG/CR-3814, ORNL/TM-9166, U.S. Nuclear Regulatory Commission, Washington, DC, 1984.
13. F. W. Stallmann, Statistical Evaluation of the Metallurgical Test Data in the ORR-PSF-PVS Irradiation Experiment, NUREG/CR-3815, ORNL/TM-9207, U.S. Nuclear Regulatory Commission, Washington, DC, 1984.
14. Regulatory Guide 1.99, Effects of Residual Elements on Predicted Radiation Damage to Reactor Vessel Materials, Rev. 1, U.S. Nuclear Regulatory Commission, Washington, DC, 1977.
15. G. L. Guthrie, "Charpy Trend Curves Based on 177 PWR Data Points," LWR-PV-SDIP Quarterly Progress Report, April-June 1983, NUREG/CR-3391, Vol. 2, U.S. Nuclear Regulatory Commission, Washington, DC, 1983.
16. P. N. Randall, "Regulatory Position," Attachment to the Minutes of the ASTM E10.02 Meeting, (draft), San Diego, CA, January 1984.

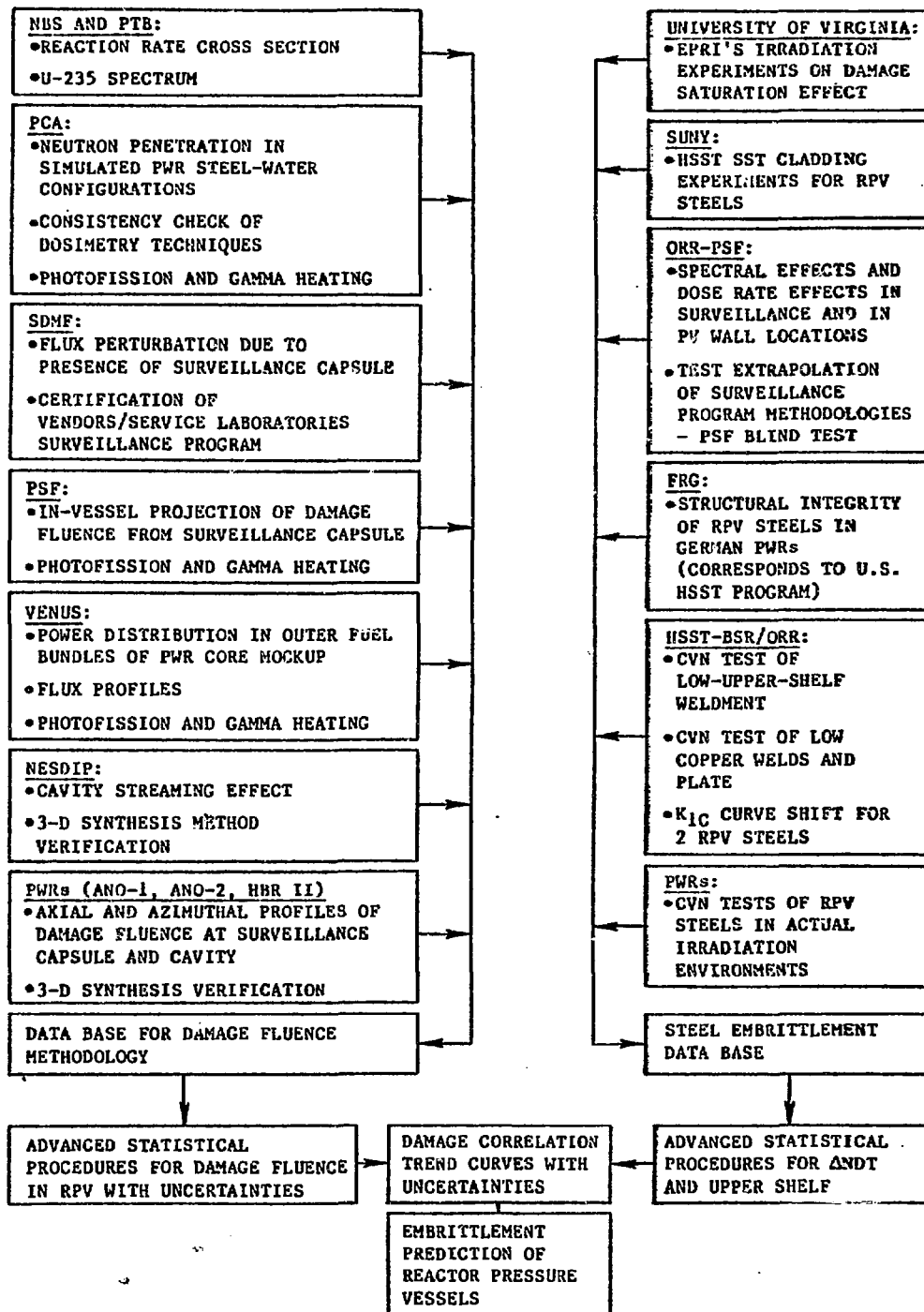


Fig. 1. Benchmark experiments in the framework of the LWR Surveillance Dosimetry Improvement Program.

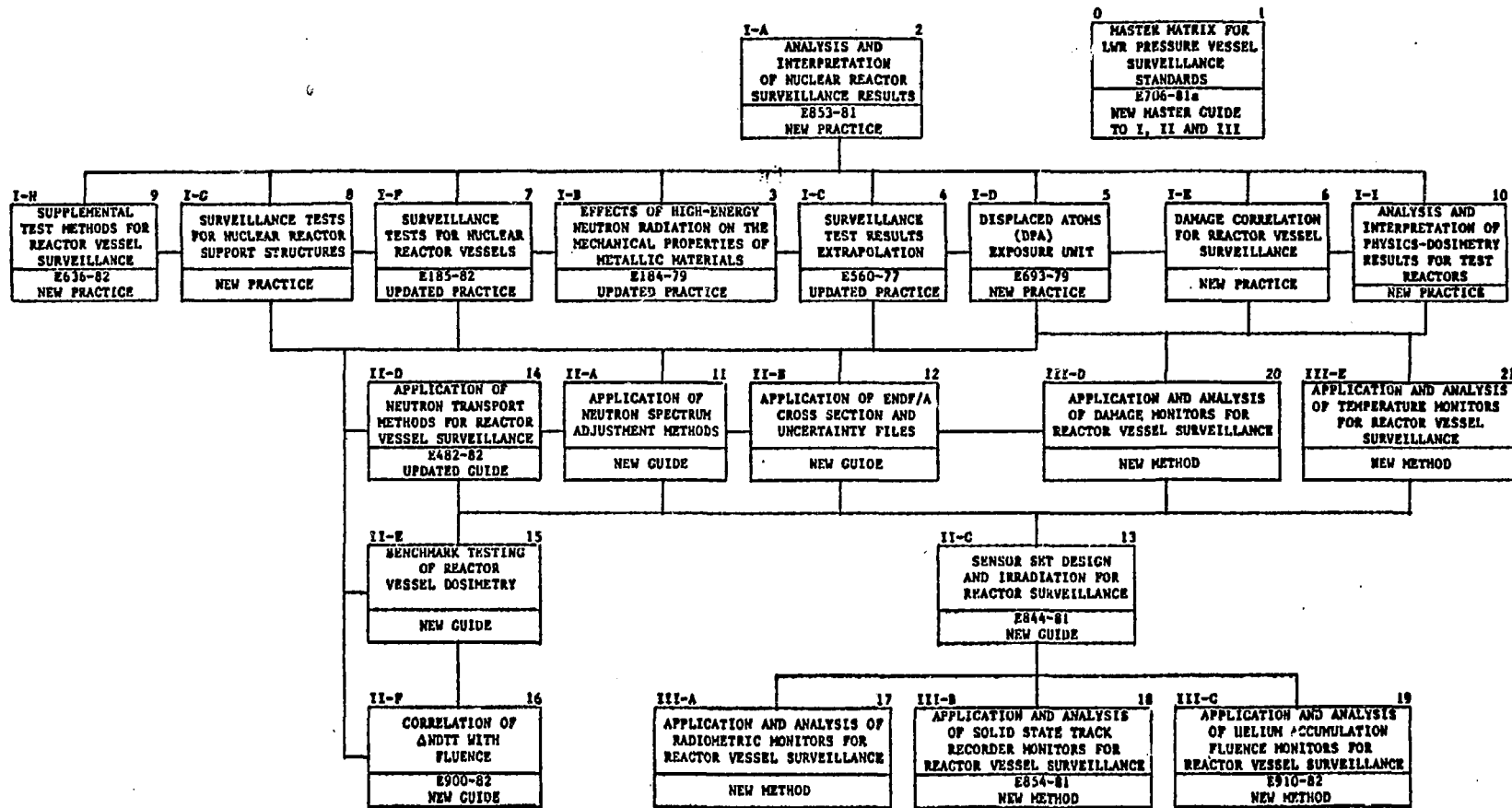


Fig. 2. ASTM Standards for surveillance of nuclear reactor pressure vessels.

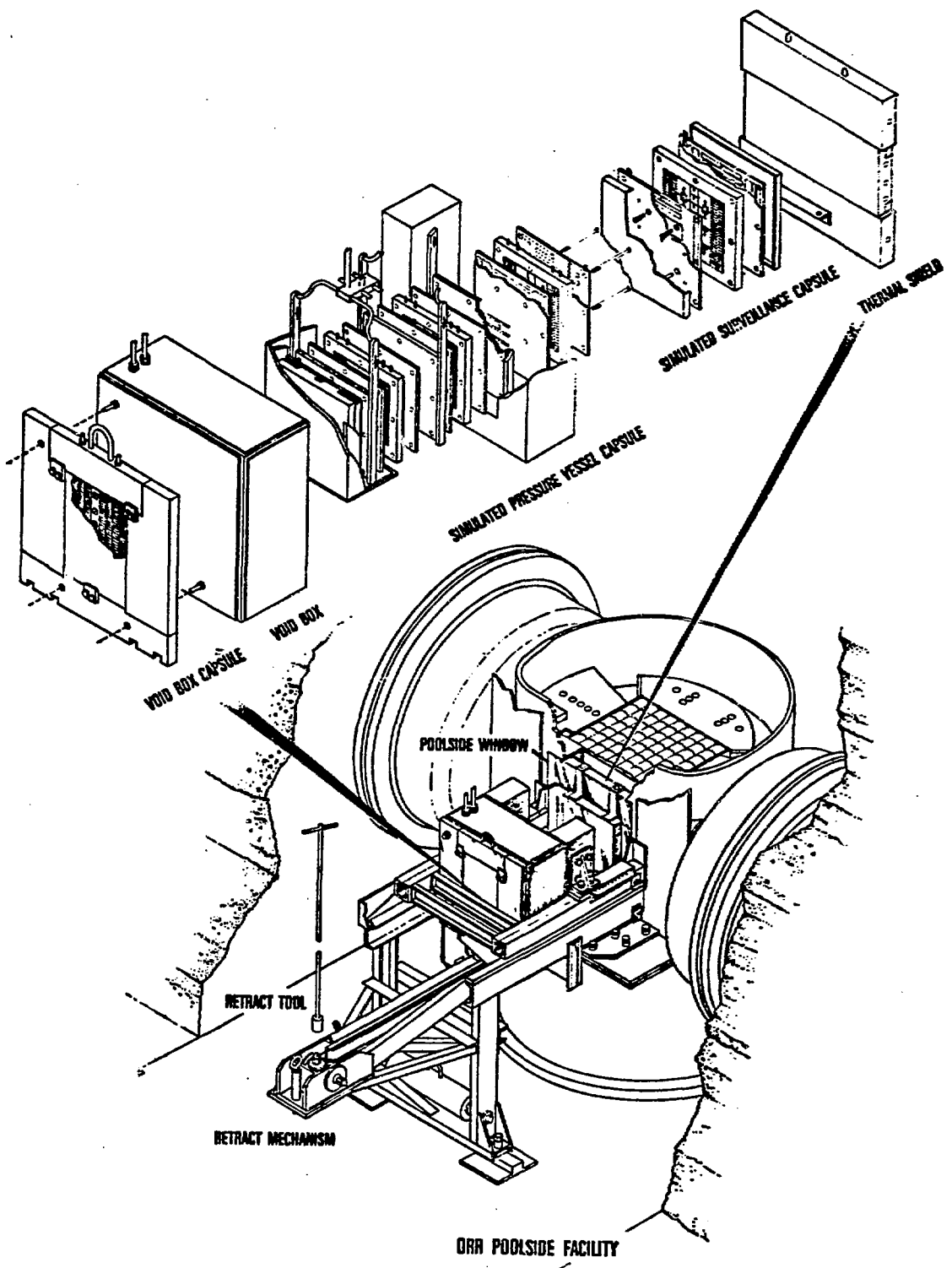


Fig. 3. ORR-PSF Irradiation Facility.

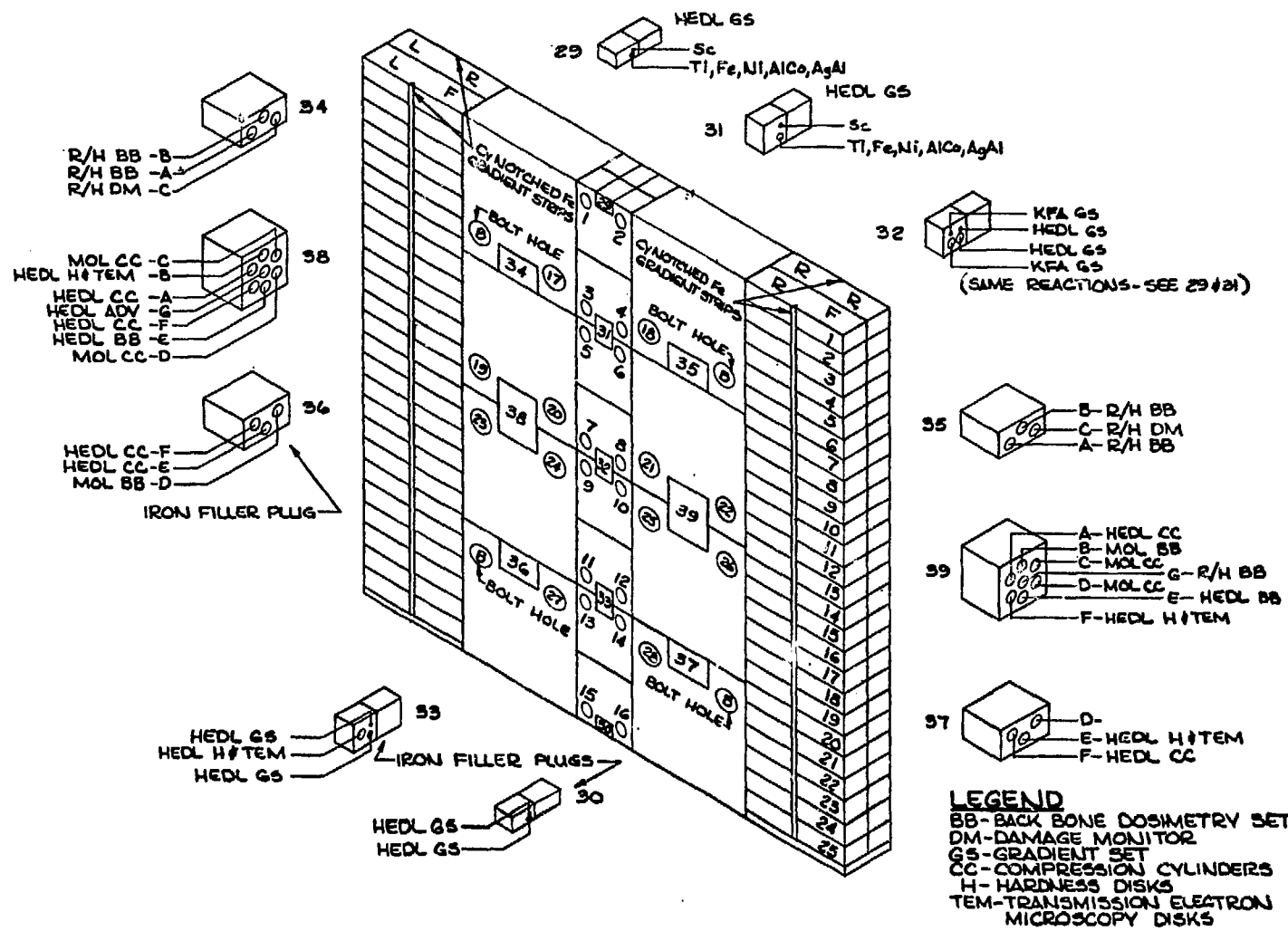


Fig. 4. Illustration of a typical dosimeter and metallurgical specimen assembly in the irradiation capsules.

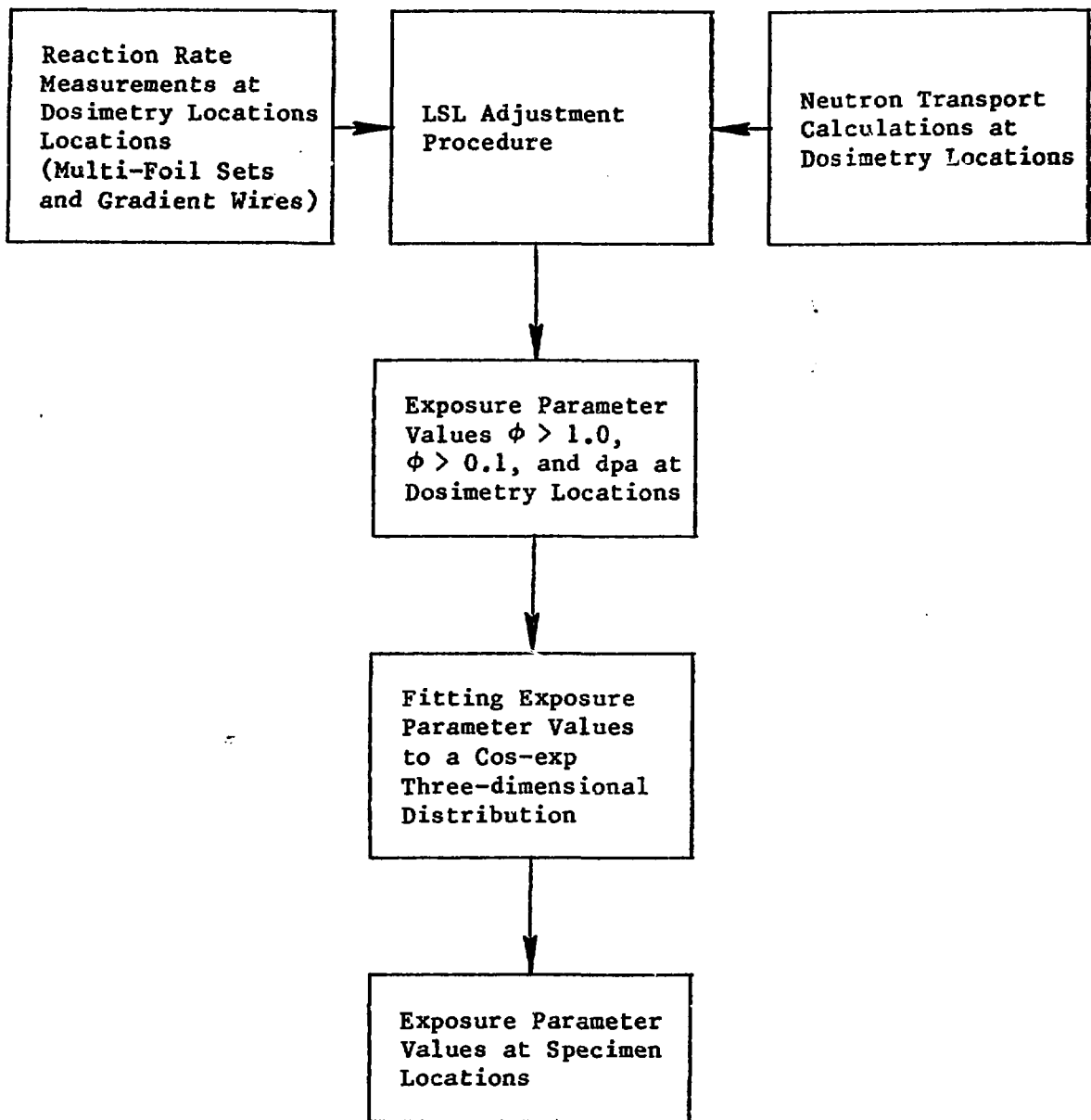


Fig. 5. Methodology for the determination of exposure parameter values and uncertainties.

ORNL DWG. 84-9111

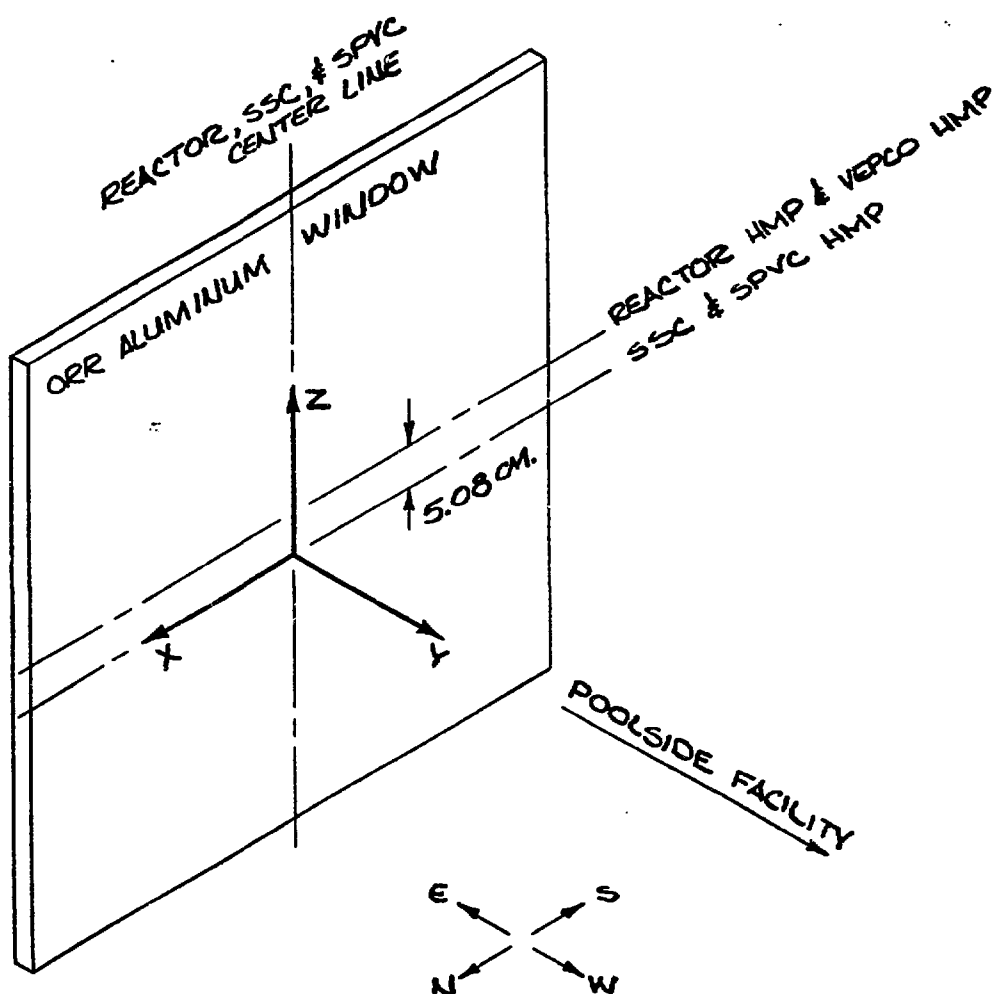
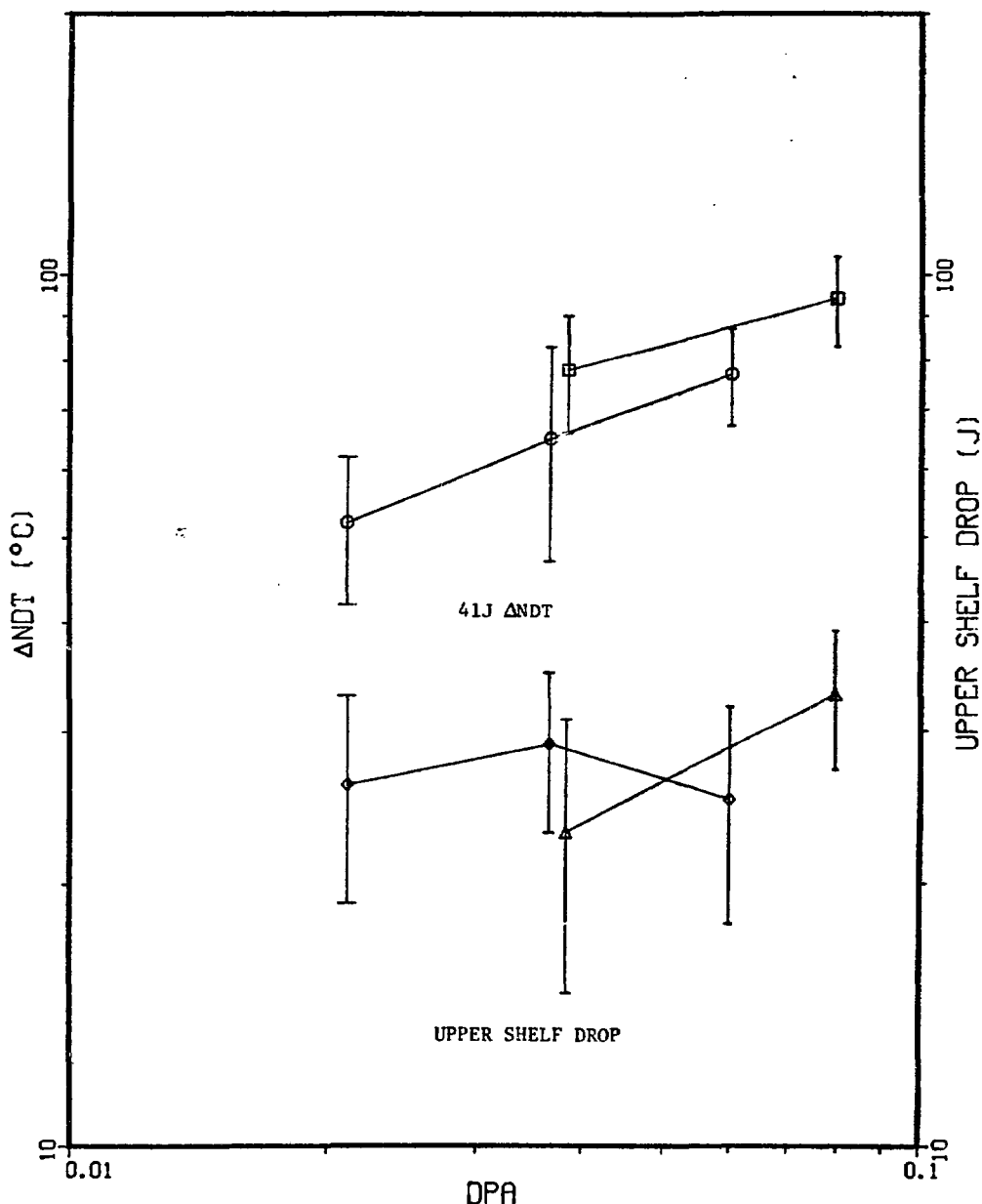


Fig. 6. Coordinate system for the ORR-PSF metallurgical experiment.

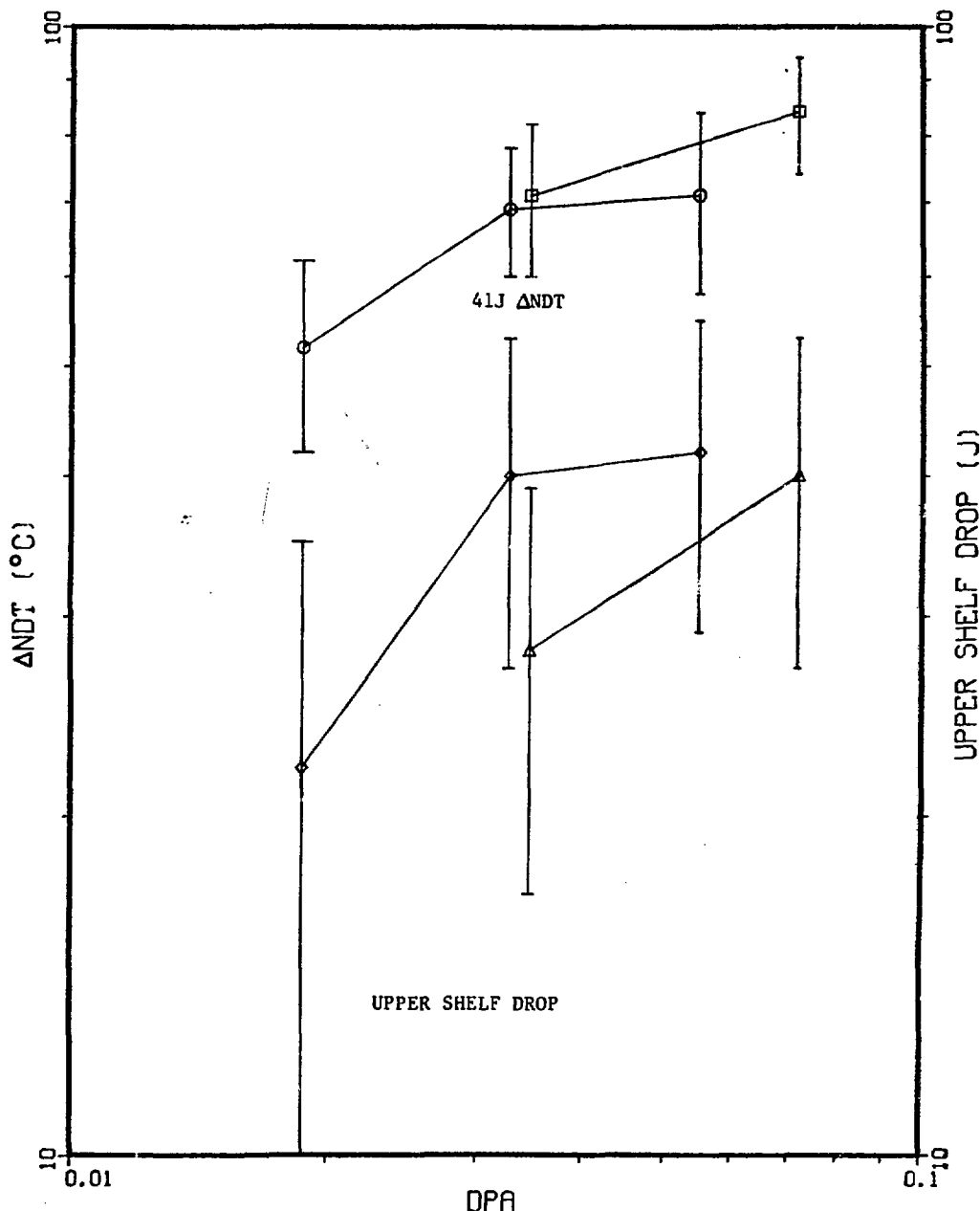
A302-B PLATE

- - 41J Δ NDT - SSC
- - 41J Δ NDT - SPVC
- △ - UPPER SHELF DROP - SSC
- ◊ - UPPER SHELF DROP - SPVC

Fig. 7. Δ NDT and upper shelf drop vs. dpa, A302-B plate.

A533-B PLATE

- - 41J Δ NDT - SSC
- - 41J Δ NDT - SPVC
- △ - UPPER SHELF DROP - SSC
- ◊ - UPPER SHELF DROP - SPVC

Fig. 8. Δ NDT and upper shelf drop vs. dpa, A533-B plate.

22NiMoCr37 FORGING

□ - 68J Δ NDT - SSC
 ○ - 68J Δ NDT - SPVC
 △ - UPPER SHELF DROP - SSC
 ◇ - UPPER SHELF DROP - SPVC

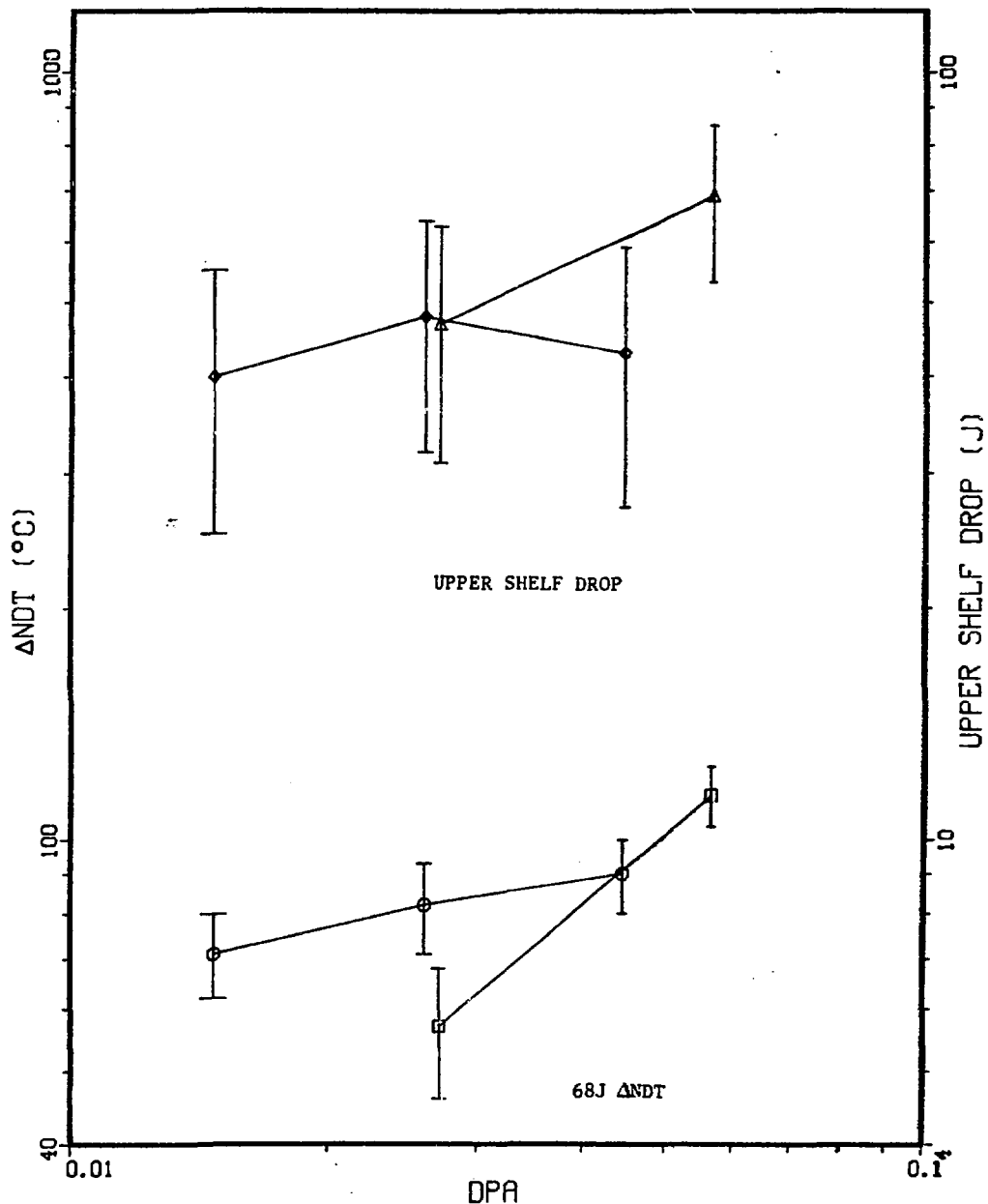
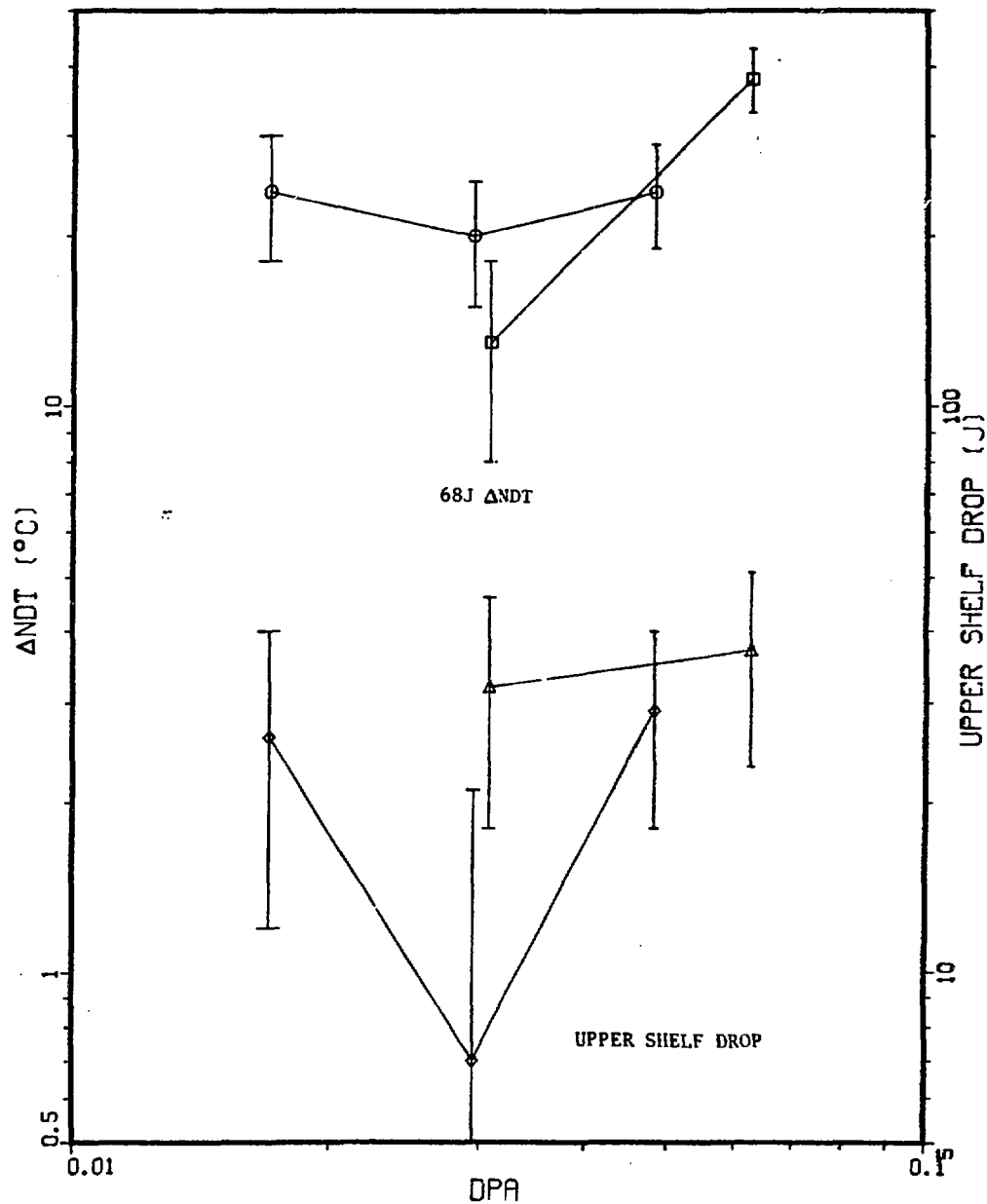


Fig. 9. Δ NDT and upper shelf drop vs. dpa, 22NiMoCr37 forging.

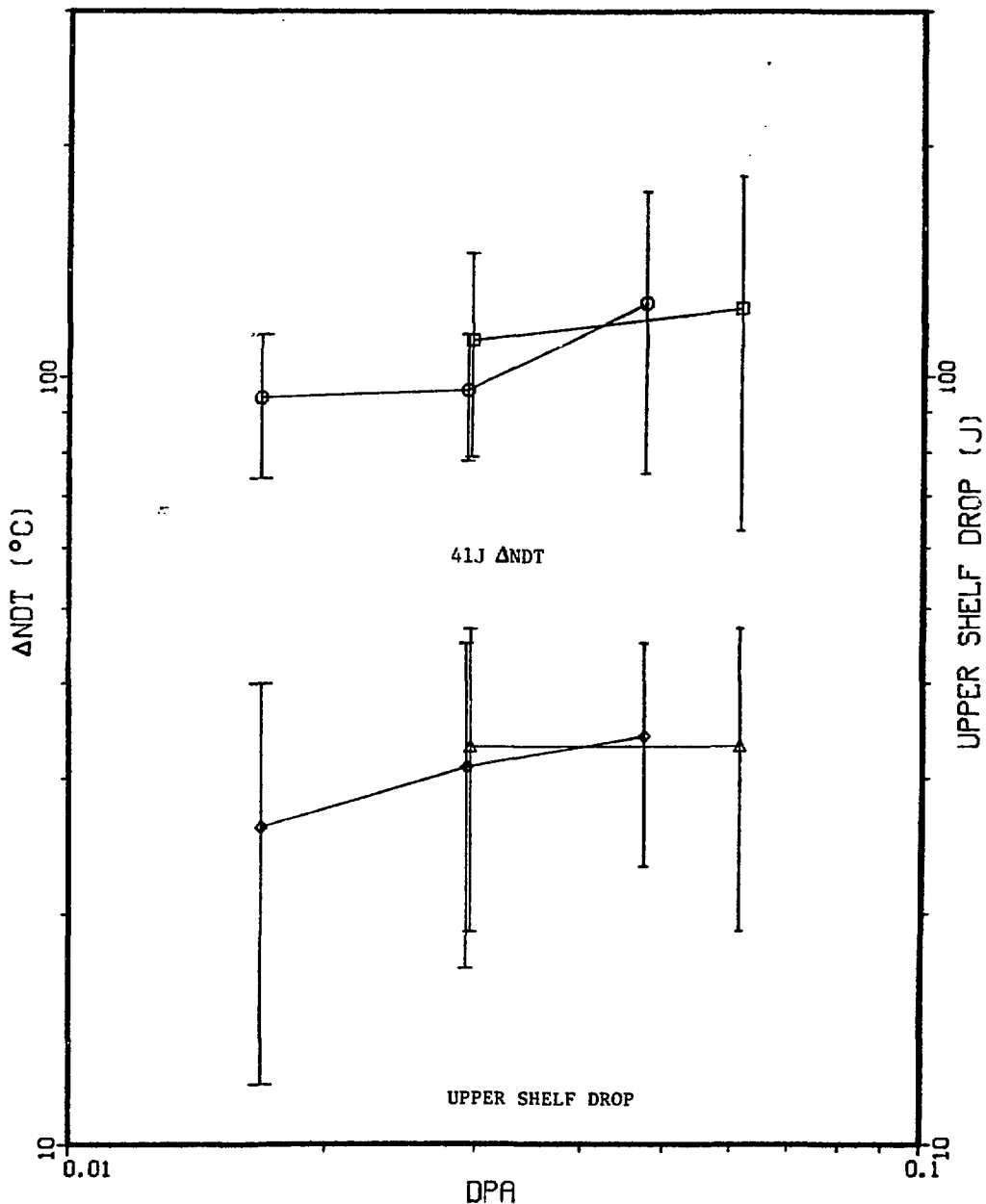
A508-3 FORGING

- - 68J Δ NDT - SSC
- - 68J Δ NDT - SPVC
- △ - UPPER SHELF DROP - SSC
- ◊ - UPPER SHELF DROP - SPVC

Fig. 10. Δ NDT and upper shelf drop vs. dpa, A508-3 forging.

SUBMERGED ARC WELD (EC)

□ - 41J Δ NDT - SSC
 ○ - 41J Δ NDT - SPVC
 △ - UPPER SHELF DROP - SSC
 ◇ - UPPER SHELF DROP - SPVC

Fig. 11. Δ NDT and upper shelf drop vs. dpa, submerged arc weld (EC).

SUBMERGED ARC WELD (R)

□ - 41J Δ NDT - SSC
 ○ - 41J Δ NDT - SPVC
 △ - UPPER SHELF DROP - SSC
 ◇ - UPPER SHELF DROP - SPVC

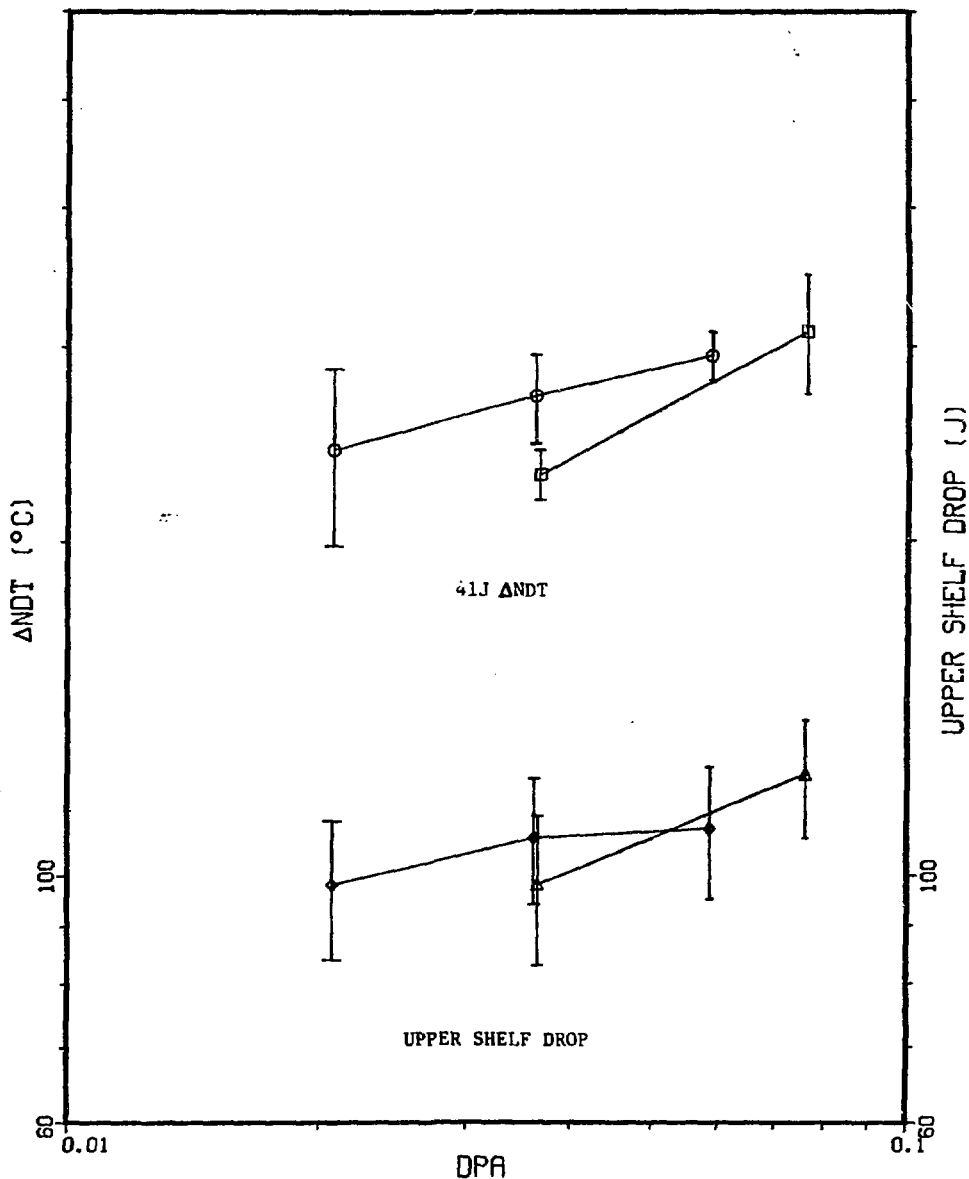


Fig. 12. Δ NDT and upper shelf drop vs. dpa, submerged arc weld (R).

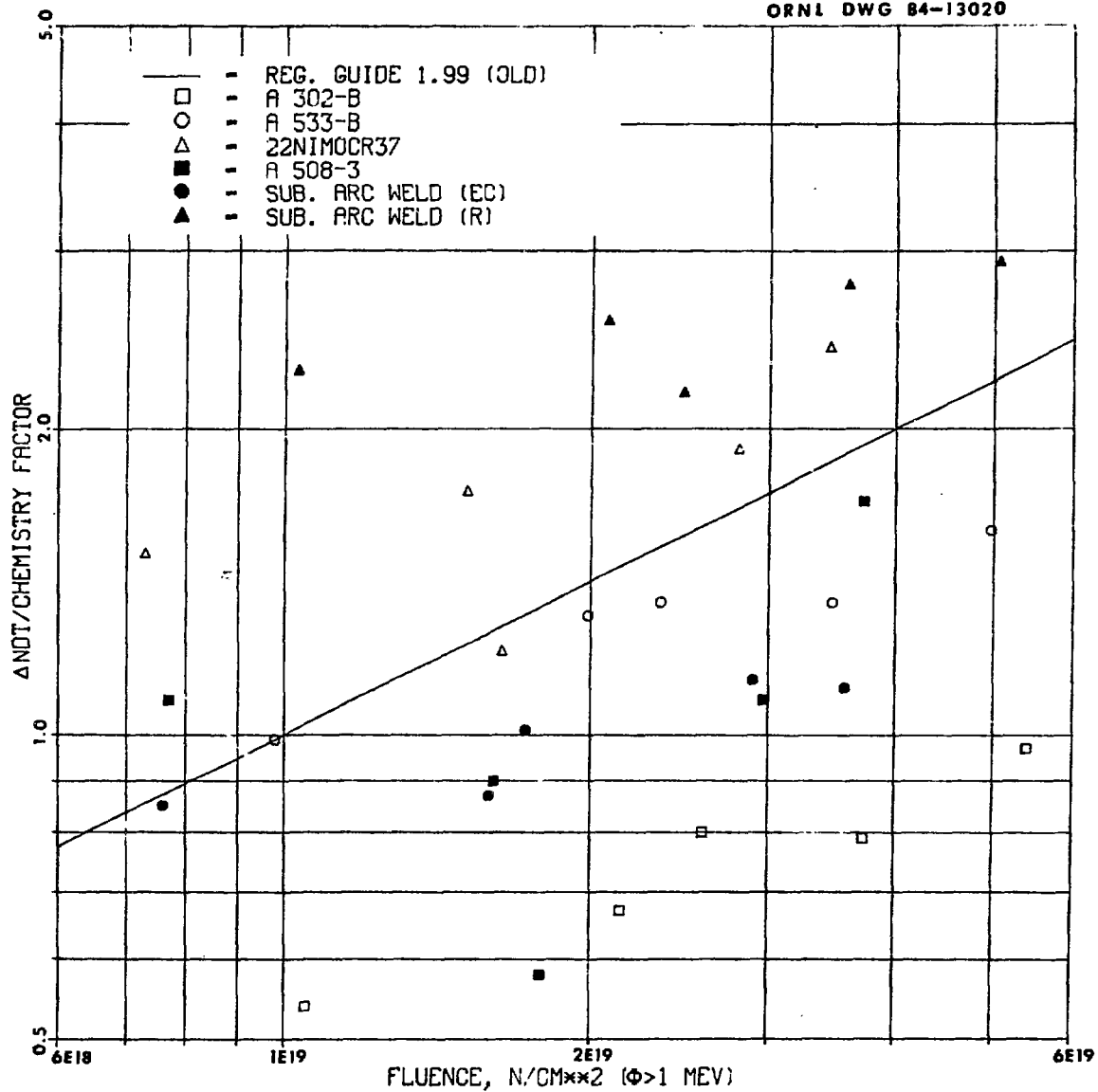


Fig. 13. Positions of ORR-PSF Charpy data relative to Reg. Guide 1.99. Data are adjusted for chemistry factors. Data above the line are underpredicted.

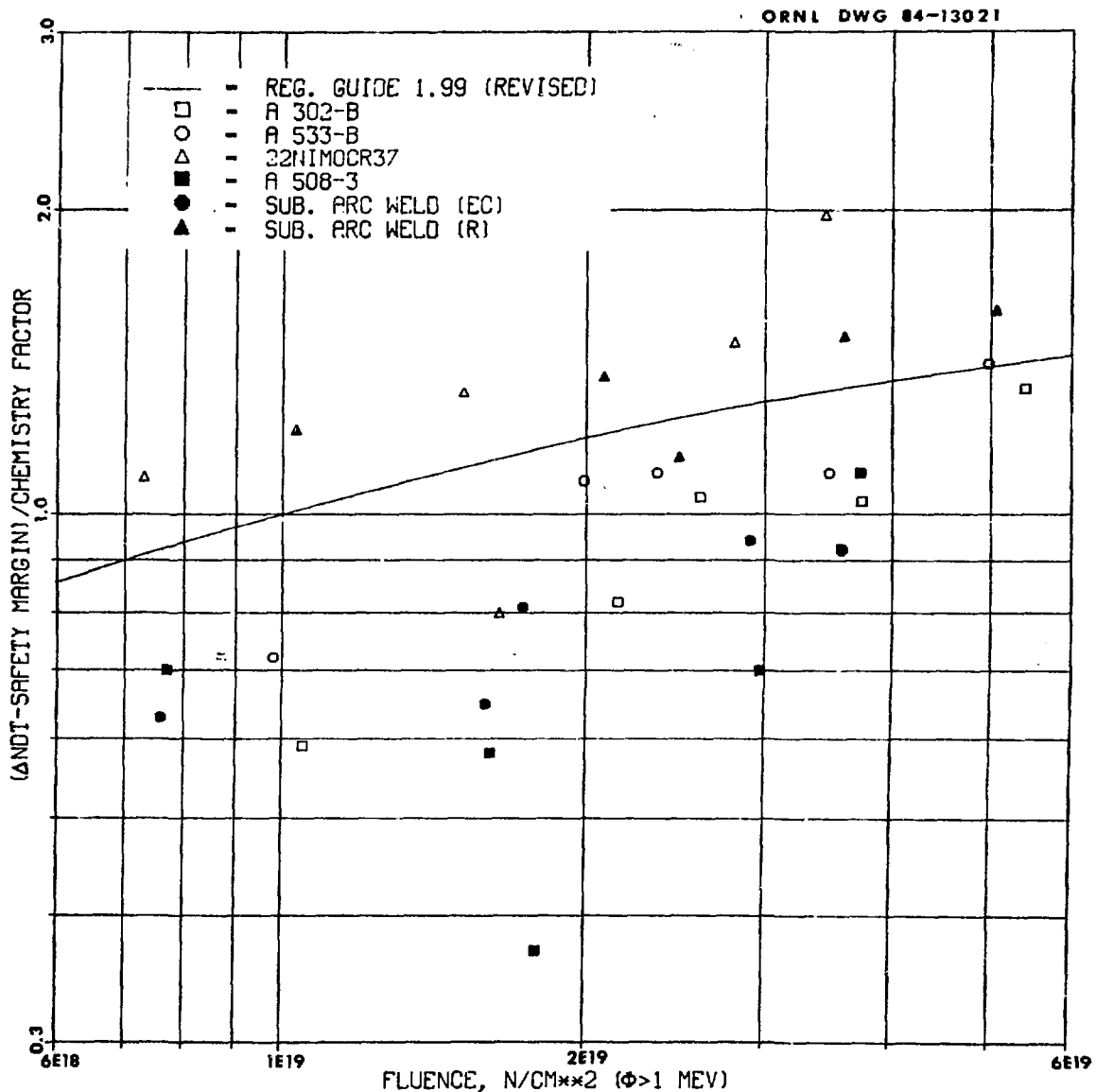


Fig. 14. Positions of ORR-PSF Charpy data relative to the revised Reg. Guide 1.99 (Guthrie formula). Data are adjusted for chemistry factors, and safety margin is added. Data above the line exceed predictions including safety margin.

Table 1. Fluences and dpa at capsule centers

		$\phi > 1.0$ Std.	$\phi > 0.1$ Std.	$\phi < 0.4$ Std.	ϕ_{total} Std.	dpa Std.					
		MeV	MeV	eV	dev.	dev.	dev.				
		(%)	(%)	(%)	(%)	(%)	(%)				
<u>SSC1</u>	H4	2.56*	5.1	7.74	5.8	1.26	7.4	14.20	5.8	4.07	4.9
<u>SSC2</u>	H9	5.50	5.1	16.84	5.8	2.79	7.4	30.55	5.5	8.80	4.9
<u>O-T</u>	H14	4.10	5.1	12.26	5.8	6.29	7.6	27.66	5.8	6.56	4.9
<u>1/4T</u>	H19	2.21	5.2	8.98	6.0	0.84	7.9	14.75	5.5	4.13	5.2
<u>1/2T</u>	H24	1.05	5.4	5.83	6.0	0.27	8.3	9.17	5.6	2.39	5.4

*Read values for $\phi > 1.0$ MeV, $\phi > 0.1$ MeV, $\phi < 0.4$ eV, and ϕ_{total} as 2.56×10^{19} neutrons/cm², etc.

Table 2. Fitting parameters for formula (1)

	P_0^*	B_X	X_0	B_Z	Z_0	λ	Y_0
		(cm ⁻¹)	(cm)	(cm ⁻¹)	(cm)	(cm ⁻¹)	(cm)
<u>SSC1</u>							
$\phi t > 1.0$ MeV	2.500E+19	0.0499	0.41	0.0436	0.97	0.176	13.29
$\phi t > 0.1$ MeV	7.607E+19	0.0507	0.37	0.0464	0.80	0.134	13.29
dpa	3.995E-02	0.0502	0.38	0.0449	0.90	0.156	13.29
<u>SSC2</u>							
$\phi t > 1.0$ MeV	5.341E+19	0.0528	-0.95	0.0457	0.03	0.176	13.29
$\phi t > 0.1$ MeV	1.648E+20	0.0539	-0.88	0.0484	-0.02	0.134	13.29
dpa	8.580E-02	0.0533	-0.91	0.0470	0.02	0.156	13.29
<u>O-T</u>							
$\phi t > 1.0$ MeV	3.924E+19	0.0517	-0.69	0.0395	0.72	0.107	24.05
$\phi t > 0.1$ MeV	1.214E+20	0.0522	-0.64	0.0432	0.71	0.042	24.05
dpa	6.452E-02	0.0516	-0.67	0.0414	0.71	0.079	24.05
<u>1/4T</u>							
$\phi t > 1.0$ MeV	2.143E+19	0.0478	-0.96	0.0378	1.30	0.134	28.56
$\phi t > 0.1$ MeV	8.823E+19	0.0486	-0.86	0.0425	1.14	0.070	28.56
dpa	4.037E-02	0.0481	-0.91	0.0407	1.21	0.097	28.56
<u>1/2T</u>							
$\phi t > 1.0$ MeV	1.016E+19	0.0441	-0.94	0.0349	1.94	0.146	33.70
$\phi t > 0.1$ MeV	5.727E+19	0.0452	-0.79	0.0413	1.48	0.089	33.70
dpa	2.333E-02	0.0450	-0.83	0.0395	1.59	0.107	33.70

*Values for $\phi t > 1.0$ MeV and $\phi t > 0.1$ MeV are in neutrons/cm².

Table 3. List of materials and chemical compositions (wt-%)

Material	Heat code	Supplier	P	Ni	Cu
A302-B (ASTM reference plate)	F23	NRL	0.011	0.18	0.20
A533-B (HSST plate 03)	3PS, 3PT, 3PU	NRL	0.011	0.56	0.12
22NiMoCr37 forging	K	KFA	0.009	0.96	0.12
A508-3 forging	MO	MOL	0.008	0.75	0.05
Submerged arc weld (single vee type, A533-B base plate)	EC	EPRI	0.007	0.64	0.24
Submerged arc weld (single vee type A533-B base plate)	R	Rolls-Royce & Assoc. Ltd.	0.009	1.58	0.23

Table 4. Summary of radiation damage determinations for the Charpy specimen

	$\dot{\tau} > 1.0 \text{ MeV}$ ($\text{n/cm}^2 \cdot 10^{19}$)*	$\dot{\tau} > 0.1 \text{ MeV}$ ($\text{n/cm}^2 \cdot 10^{19}$)	dpa	ΔNDT 41J (°C)	Std. dev.	ΔNDT 68J (°C)	Std. dev.	ΔNDT 0.89 mm (°C)	Std. dev.	Upper shelf drop (J)	Std. dev. (J)
<u>A-302-B</u>											
SSC1	2.59	7.46	3.86	78	± 12	84	± 17	86	± 10	23	± 8
SSC2	5.38	15.35	7.96	94	± 11	(101)**	± 15	92	± 10	33	± 6
0-T	3.95	11.44	6.06	77	± 10	(87)	± 20	(77)	± 16	25	± 7
1/4 T	2.16	8.13	3.70	65	± 18	(109)	± 83	(72)	± 15	29	± 6
1/2 T	1.03	5.27	2.11	52	± 10	(57)	± 17	56	± 10	26	± 7
<u>A-533-B</u>											
SSC1	2.32	6.61	3.44	71	± 11	71	± 12	85	± 9	28	± 11
SSC2	4.83	13.63	7.11	84	± 10	86	± 11	91	± 7	40	± 13
0-T	3.59	10.20	5.46	71	± 13	(92)	± 25	91	± 10	42	± 13
1/4 T	1.95	7.13	3.28	69	± 9	65	± 7	74	± 6	40	± 13
1/2 T	0.94	4.60	1.87	52	± 10	52	± 8	57	± 7	22	± 13
<u>22NIMOCR37</u>											
SSC1	1.75	5.69	2.77	(52)	± 16	57	± 11	78	± 7	47	± 16
SSC2	3.64	11.70	5.72	109	± 14	114	± 10	117	± 8	69	± 16
0-T	2.71	8.77	4.40	81	± 16	90	± 10	97	± 7	43	± 16
1/4 T	1.47	6.11	2.64	66	± 18	82	± 11	93	± 8	48	± 16
1/2 T	0.71	3.97	1.51	66	± 13	71	± 9	74	± 8	40	± 15
<u>A-508-3</u>											
SSC1	1.93	6.32	3.07	15	± 7	13	± 5	18	± 5	32	± 14
SSC2	4.02	13.02	6.34	39	± 7	38	± 5	38	± 5	37	± 14
0-T	2.95	9.65	4.80	27	± 7	24	± 5	26	± 5	29	± 11
1/4 T	1.60	6.84	2.92	23	± 6	20	± 5	23	± 5	7	± 14
1/2 T	0.77	4.45	1.67	22	± 7	24	± 6	21	± 6	26	± 14
<u>Submerged arc weld (EC)</u>											
SSC1	1.87	6.11	2.97	112	± 33	(166)	± 120	(142)	± 35	33	± 14
SSC2	3.90	12.59	6.14	123	± 60	(157)	-	138	± 20	33	± 14
0-T	2.88	9.45	4.71	125	± 50	-	-	(171)	± 66	34	± 11
1/4 T	1.60	6.82	2.92	96	± 18	-	-	(118)	± 22	31	± 14
1/2 T	0.77	4.48	1.68	94	± 20	(136)	± 65	(129)	± 42	26	± 14
<u>Submerged arc weld (R)</u>											
SSC1	2.46	7.07	3.66	230	± 12	259	± 21	260	± 17	98	± 15
SSC2	5.13	14.56	7.57	309	± 38	-	-	352	± 64	123	± 15
0-T	3.81	10.97	5.83	294	± 15	-	-	(364)	± 96	110	± 15
1/4 T	2.12	7.05	3.62	270	± 25	-	-	(321)	± 58	108	± 14
1/2 T	1.02	5.21	2.09	242	± 44	-	-	270	± 22	98	± 14

 *neutrons/cm²·10¹⁹,

**values in parentheses are obtained by extrapolation and may be unreliable.

Table 5. Comparison between experimentally determined Charpy shift and Blind Test predictions

	Determined from Charpy curves			Smallest and largest values predicted by Blind Test participants		Difference Blind Test - CV81	
	CV81*	Std.	MEA**	Min.	Max.	Min.	Max.
	(°C)	(°C)	(°C)	(°C)	(°C)	(°C)	(°C)
<u>A302-B</u>							
SSC1	78	+12	82	71	98	-7	+20
SSC2	94	+11	94	75	112	-19	+18
0-T	77	+10	81	71	96	-6	+19
1/4T	65	+18	67	65	81	0	+16
1/2T	52	+10	50	45	66	-7	+14
<u>A533-B</u>							
SSC1	71	+11	61	45	69	-24	-2
SSC2	84	+10	81	62	99	-22	+15
0-T	71	+13	75	60	87	-11	+16
1/4T	69	+ 9	69	54	63	-15	-6
1/2T	52	+10	53	26	52	-26	0
<u>22NiMoCr37</u>							
SSC1	52	+16	61	57	77	-5	+25
SSC2	109	+14	94	65	110	-44	+1
0-T	81	+16	72	63	97	-18	+16
1/4T	66	+18	78	52	76	-14	+10
1/2T	66	+13	56	45	64	-21	-2
<u>A508-3</u>							
SSC1	15	+ 7	20	6	43	-9	+18
SSC2	39	+ 7	39	11	53	-28	+14
0-T	27	+ 7	25	10	49	-17	+22
1/4T	23	+ 6	20	8	42	-15	+19
1/2T	22	+ 7	14	6	35	-16	+13
<u>Submerged arc weld (EC)</u>							
SSC1	112	+33	108	99	118	-13	+6
SSC2	123	+60	119	130	153	-7	+30
0-T	125	+50	124	121	135	-4	+10
1/4T	96	+18	94	91	115	-5	+19
1/2T	94	+20	89	63	103	-31	+9
<u>Submerged arc weld (R)</u>							
SSC1	230	+12	222	218	227	-12	-3
SSC2	309	+38	289	246	319	-63	+10
0-T	294	+15	286	239	288	-55	-6
1/4T	270	+25	256	180	218	-90	-52
1/2T	242	+44	239	143	189	-99	-53

*ORNL evaluation.

**Evaluation in Ref. 4.